Surface vs bulk contribution to the second-harmonic generation in AlGaAs nanoresonators

Yigong Luan[1,*], *Agostino* Di Francescantonio[1], *Attilio* Zilli[1], *Davide* Rocco[2], *Vincent* Vinel[3], *Adrien* Borne[3], *Aristide* Lemaître[4], *Paolo* Biagioni[1], *Lamberto* Duò[1], *Marco* Finazzi[1], *Costantino* De Angelis[2], *Giuseppe* Leo[3], and *Michele* Celebrano[1]

[1]Physics Department, Politecnico di Milano, Piazza Leonardo Da Vinci 32, 20133 Milano, Italy
[2]Department of Information Engineering, University of Brescia, Via Branze 38, 25123 Brescia, Italy
[3]Université de Paris, CNRS, Laboratoire Matériaux et Phénomènes Quantiques, 75013 Paris, France
[4]Centre de Nanosciences et de Nanotechnologies, CNRS, Université Paris-Saclay, 91120 Palaiseau, France

Abstract. We address the surface vs bulk origin of the second-order optical nonlinearity in AlGaAs nanocylinders through polarization-resolved measurements. By comparing numerical simulations accounting just for bulk second-order nonlinearity with experimental results, we show that the surface contribution to second-harmonic generation (SHG) cannot be neglected and depends on the resonant conditions of the nanocylinder. Additionally, our analysis suggests that bulk and surface SHG are competing effects, and that their interference might influence the overall efficiency.

1 Introduction

At the nanoscale nonlinear optical processes become inherently weak because of the reduced amount of matter involved. However, it has been recently shown that such a limitation can be partially compensated by exploiting the field enhancement at the operating frequencies (fundamental and harmonic) associated with Mie resonances in dielectric nanoantennas. One of the major advantages of many dielectric materials is the negligible optical losses in the near and medium infrared range. In this framework, III–V semiconductors and ionic crystals often have a large bulk nonlinear susceptibility, thanks to their non-centrosymmetric crystal structures, and can sustain strong Mie resonances. In such systems, the bulk contribution to second-harmonic generation (SHG) often becomes dominant [1]. However, some recent works reported that in some cases the surface contribution to SHG in non-centrosymmetric materials can be comparable to the bulk one [2]. In this work, we investigate dielectric nanocylinders made of $Al_{0.18}Ga_{0.82}As$ to investigate the surface contribution to SHG. $Al_{0.18}Ga_{0.82}As$ exhibits a large second-order susceptibility and a broad optical transparency window, which can significantly suppress two-photon absorption and prevent SH reabsorption in the near-infrared range [3]. The dependence of SHG on the polarization of the illumination at the fundamental wavelength is studied to reveal surface contributions, and it is carried out systematically on a set of nanoantennas with variable radii from 183 nm to 207 nm with steps of 6 nm around the magnetic dipole resonance [4].

2 Results and discussion

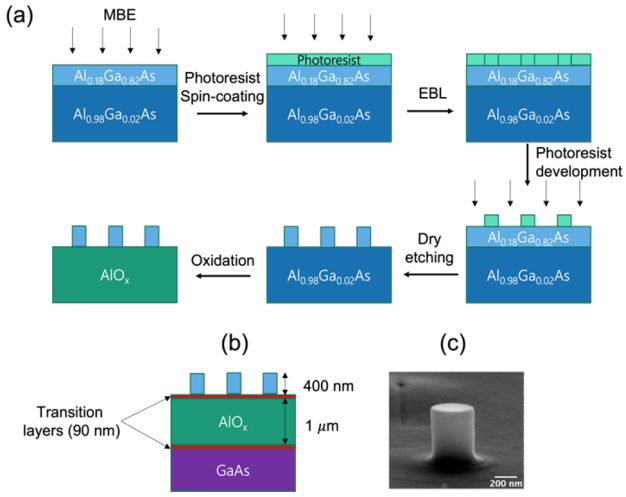

Fig. 1. (a) Fabrication process and selection of single nanocylinders of monolithic AlGaAs-on-AlOx platform. (b) cross-sectional view of the structure of the sample. (c) tilted-view scanning electron micrograph of a single nanocylinder.

The fabrication process and the resulting sample are sketched in Figure 1. Firstly, we utilized molecular beam epitaxy to deposit a layer of 400 nm-thick $Al_{0.18}Ga_{0.82}As$ on the top of an aluminium-rich substrate. A thin layer of photoresist was then spin-coated on top and patterned by means of e-beam lithography. Then the sample was dry etched to fabricate arrays of cylinders and expose the aluminium-rich substrate. In the end, the substrate was oxidized to form a 1 μm-thick AlO_x layer (n = 1.6). Our sample consists in a set of arrays of 3 μm-spaced

* Corresponding author: yigong.luan@polimi.it

$Al_{0.18}Ga_{0.82}As$ nanocylinders with a radius that ranges between 165 nm and 365 nm and a height of 400 nm.

In our experiment, an ultrafast (160 fs) laser delivers pulses with a 1550 nm central wavelength and an 80 MHz repetition rate. The beam is tightly focused on the sample with a microscope air objective (0.70 numerical aperture). The SHG emission is collected by the same objective, chromatically filtered, and detected by a single-photon avalanche diode. We have also performed numerical simulations considering cylinders surrounded by air (n = 1.0) on a 1 μm-thick AlOx (n = 1.6) thin film on top of a GaAs substrate. The internal field distribution at the fundamental frequency is computed in the frequency domain by COMSOL Multiphysics. Then, the SHG is evaluated by considering just the bulk nonlinear susceptibility $\chi^{(2)}_{\mathrm{bulk}}$.

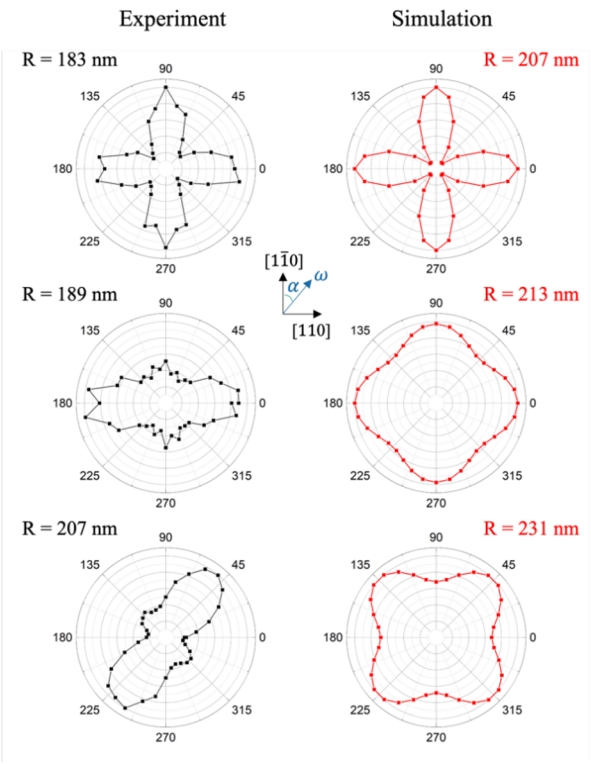

Fig. 2. Measured and simulated normalized SHG emission at different nanocylinder radii R as a function of the linear polarization of the impinging illumination at the fundamental frequency. The polar plots on the left (black) represent the measured SHG at R = 183 nm, R = 189 nm, and R = 207 nm. The polar plots on the right (red) display calculated SHG at R = 207 nm, R = 213 nm, and R = 231 nm.

Figure 2 presents a comparison between measured and numerically calculated SHG for three distinct radii. The experimentally acquired SHG polar plots are averaged on five nominally identical single cylinders to average out possible statistical deviations due to fabrication defects. A nearly four-fold symmetry of SHG emission is observed at the radius of 183 nm, indicating a dominant bulk contribution. In fact, the local maxima correspond to a pump polarization aligned with the material crystallographic axes as both axes are excited equally. This is confirmed by the simulated polar plot for a nanocylinder of 207 nm radius, which exhibits a magnetic dipole resonance at the wavelength employed in the SHG experiments, as already reported in [3]. A 24 nm deviation from the nominal radius can be ascribed to fabrication tolerances and is compatible with previous observations [3]. By simulating larger radii keeping this offset fixed, we retrieve a four-fold symmetry in the polar plots for all the radii that we investigated experimentally. This is expected since the second-order bulk susceptibility tensor of AlGaAs only features non vanishing off-diagonal components that are equal in magnitude. Yet, the SHG signal obtained on cylinders with radius equal to 189 nm and 207 nm, a significant reduction of the symmetry of the emission pattern is observed, the four-fold symmetry being turned into a two-fold symmetry. As already pointed out in previous works [2], this behaviour can bear the signature of a non-negligible contribution from the surface, which interferes with the bulk contribution of SHG. We stress the fact that, for the larger nanocylinder (207 nm), besides the marked difference in symmetry of the polar plot ascribed to surface effects, both simulation and experiment feature a 45° rotation of the polar plot, indicating the presence of a different resonant mode.

3 Conclusions

We have investigated individual $Al_{0.18}Ga_{0.82}As$ nanoantennas by polarization-resolved excitation measurements. We ascribe the observed deviation from the simulations, which consider only a bulk contribution to the SHG process, to a potential surface contribution, which still needs to be further verified. We found that, depending on the excitation wavelength, the surface contribution can be either negligible or comparable to the bulk effects. This interplay between bulk and surface effects based on these platforms must be considered as a potential reason why the real-world performance of nano-optical systems may deviate from the design predictions. In addition, the presence of non-negligible surface SHG can be relevant for applications such as sensing, which might benefit from the increased surface sensitivity of the SHG process.

References

1. A. Tognazzi, P. Franceschini, D. Rocco, L. Carletti, A. Locatelli, M. Gandolfi, D. Zappa, A.C. Cino, E. Comini, G. Leo, C. De Angelis, IEEE Photonics Technol. Lett. **35**, 505–508 (2023)
2. S.D. Gennaro, C.F. Doiron, N. Karl, P.P. Iyer, D.K. Serkland, M.B. Sinclair, I. Brener, ACS Photonics **9**, 1026–1032 (2022)
3. V.F. Gili, L. Carletti, A. Locatelli, D. Rocco, M. Finazzi, L. Ghirardini, I. Favero, C. Gomez, A. Lemaître, M. Celebrano, C. De Angelis, G. Leo, Opt. Express **24**, 15965–15971 (2016)
4. L. Ghirardini, L. Carletti, V. Gili, G. Pellegrini, L. Duò, M. Finazzi, D. Rocco, A. Locatelli, C. De Angelis, I. Favero, M. Ravaro, G. Leo, A. Lemaître, and M. Celebrano, Opt. Lett. **42**, 559–562 (2017)